Journal of Basics and Applied Sciences Research (JOBASR)
ISSN (print): 3026-9091, ISSN (online): 1597-9962
Volume 3(4) July 2025
DOI: https://dx.doi.org/10.4314/jobasr.v3i4.17

A Study on Transient flow formation in concentric porous annuli filled with porous material having variable porosity

Sulaiman A.B[1*] & Hamza M.M[2].

[1]Department of Mathematics, Federal University, Dutsin-Ma, Katsina, Nigeria

[2]Department of Mathematics, Usmanu Danfodio University, Sokoto, Nigeria
[*]Corresponding Author Email: malamsulaiman2020@gmail.com

ABSTRACT
This research explores the transient flow formation in concentric porous annuli filled with porous material having variable porosity. The study focuses on the fluid flow between two horizontal concentric cylinders, assuming the fluid is viscous and incompressible. To solve the governing partial differential equation, the Laplace transform technique is applied, transforming it into an ordinary differential equation in the Laplace domain. Exact solutions are obtained in the Laplace domain, and then inverted to the time-dependent domain using the Riemann-sum approximation method. The accuracy of the Riemann-sum approximation method is validated by comparing the numerical values obtained with those of the exact solution for steady-state flow and transient solution. The results are presented graphically, illustrating the variations of velocity and skin friction with respect to the Darcy number and suction/injection parameter. The study reveals that suction accelerates the flow, while injection retards it. The Darcy number, which represents the permeability of the porous medium, significantly affects the flow characteristics. The skin friction, which is a measure of the shear stress at the surface, is also influenced by the suction/injection parameter. The findings of this study have implications for various engineering applications, such as groundwater flow, oil reservoirs, and chemical engineering processes. Understanding the transient flow formation in porous annuli can help optimize the design and operation of these systems. The use of the Laplace transform technique and Riemann-sum approximation method provides an efficient and accurate solution to the problem. The graphical representation of the results allows for a clear understanding of the flow characteristics and the effects of various parameters. The list of symbols, notation and meaning of parameters can be found in appendix A and B attached in section below.

Keywords:
Riemann-sum approximation,
Concentric Annuli,
Porous Material.

INTRODUCTION

The study of fluid flow in an annulus has garnered significant attention since the pioneering work of (Rothfus et al. 1950), due to its extensive applications in engineering. While fluid flow in annuli has been explored in both laminar and turbulent regimes, the transitional flow regime, particularly for non-Newtonian fluids, remains understudied. Annular flow has practical implications in various fields, including oil and gas wells, gas-cooled nuclear reactors, chemical engineering, petroleum engineering, biomedical engineering, and food processing (Kim 2013).

In drilling and production operations, annular flow plays a crucial role, especially in deviated and horizontal wells (Ebrahim et al., 2013).

The investigation of transport phenomena in porous materials has become increasingly important in engineering and environmental sciences. Porous media models have been applied to simulate complex situations, such as flow through packed and fluidized beds. Researchers have made significant contributions to understanding flow in porous media, including the effects of permeability and magnetic fields,

(Verma and Singh, 2015). Studies have also examined flow in annuli with porous walls. (Berman, 1958) have considered the steady-state laminar flow of an incompressible fluid in an annulus with porous walls. They discovered that the cross-flow (radial component of the flow) is produced by injecting fluid at one wall and removing it at the other, at equal rates. (Deo and Srivastava, 2013) studied the fully developed flow of an incompressible, electrically conducting, viscous fluid through a porous medium with variable permeability under a transverse magnetic field.

Other notable studies include analytical solutions for flow in channels partially filled with porous media (Kuznetsov 1996) and three-dimensional solutions for flow through heterogeneous porous media (Vadasz 1993). Additionally, researchers have investigated steady-state laminar flow of incompressible elastic viscous liquids in annuli with coaxial porous walls rotating about a common axis (Mishra and Roy 1967). These studies demonstrate the complexity and diversity of fluid flow in porous media and annuli, highlighting the need for continued research in this area.

The study of fluid flow in annular regions filled with porous media has been explored by various researchers. (Verma and Datta 2012) investigated the fully developed laminar flow of a viscous incompressible fluid in an annular region with variable permeability. Similarly, (Verma and Singh 2014) studied the laminar flow of a viscous incompressible fluid in an annular region with variable permeability and found that permeability variation significantly affects the flow. Other studies have examined magnetohydrodynamics (MHD) flow in annuli, such as (Jha and Apere 2013), who investigated MHD transient Couette flow in an annulus formed by two concentric porous cylinders. (Khalil et al. 2008) presented an analytical solution for steady-state fully developed one-dimensional flow in a concentric annulus with a moving core. (Jha and Apere 2012) also investigated unsteady MHD free convective flow between two concentric vertical cylinders. (Yale *et. al*., 2025) studied transverses magnetic field's impact on mixed convection flow of an Exothermic fluid over a porous material – field channel. (Kandasamy and Nadiminti 2015) studied the entrance region flow of Herschel-Bulkley fluid in concentric annuli with a rotating inner wall. Majority of real-world issues we face, particularly in the physical, social, and life sciences, may be described by using differential equations, (Sagir *at. al.*, 2023).

Additionally, researchers have explored flow in porous media under various conditions, such as (Pantokratoras and Fang 2010), who investigated fully developed flow in a fluid-saturated porous medium channel with an electrically conducting fluid. (Avramenko et al. 2015) presented results on the response of an incompressible fluid in a circular micro pipe and a parallel plate micro channel to a sudden pressure drop.

The present work focuses on transient flow formation in concentric porous annuli filled with porous material having variable porosity, which appears to be a novel contribution to the literature. The study discusses the effects of suction/injection parameter, time, and Darcy number on velocity and skin friction, using a semi-analytical method involving Laplace transformation and Riemann-sum approximation.

MATERIALS AND METHODS

In this problem, we considered the motion of a viscous, incompressible fluid in the region bounded by the porous wall of two concentric cylinders of infinite length, the z' axis is assumed to be on the axis of the porous cylinders in the horizontal direction, and r' axis is on the radial direction. The fluid exist in the region $R_1 \le r' \le R_2$ between the two porous cylinders, where R_1 and R_2 are the radii of the inner and outer cylinders, respectively. Since the cylinders are of infinite length and the flow is fully developed, all physical variables are functions of r' and t only. Fig.1 gives the schematic diagram of the problem.

The mathematical model governing the present physical situation is given as

$$\frac{\partial u'}{\partial t'} + v_0 R_1 \left[\frac{1}{r'}\frac{\partial u'}{\partial r'} + \frac{u'}{r'^2} \right] = \upsilon eff \left[\frac{\partial^2 u'}{\partial r'^2} + \frac{1}{r'}\frac{\partial u'}{\partial r'} - \frac{u'}{r'^2} \right] - \frac{\upsilon}{k} u', \tag{1}$$

Where $k = k_0 \left(\frac{r'}{R_1} \right)^2$

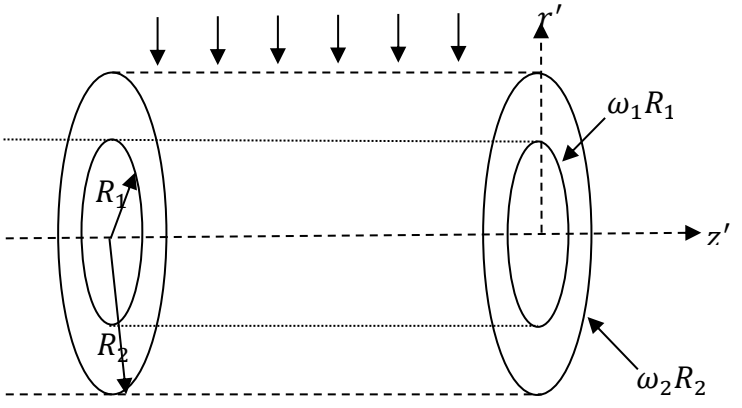

Fig.1. Schematic diagram of the problem.

The initial and boundary conditions for the problem are:

$u' = 0,\ R_1 \le r' \le R_2$ and $t' \le 0$,

$u' = \omega_1 R_1$ at $r' = R_1,\ t' > 0$,

$u' = \omega_2 R_2$ at $r' = R_2,\ t' > 0$.

With the following dimensionless quantities

$$t = \frac{t'\upsilon}{R_1^2},\ \vartheta = \frac{\upsilon_{eff}}{\upsilon},\ r = \frac{r'}{R_1},\ u = \frac{u'}{R_1\omega_1},\ \lambda = \frac{R_2}{R_1},$$
$$\theta = \frac{\omega_2}{\omega_1} \text{ And } S = \frac{v_0 R_1}{\upsilon},\ Da = \frac{k_0}{R_1^2}$$

Equation (1) can be written in dimensionless form as:

$$\frac{\partial u}{\partial t} = \vartheta\frac{\partial^2 u}{\partial r^2} + \frac{1}{r}(\vartheta - S)\frac{\partial u}{\partial r} - \frac{u}{r^2}\left[\vartheta + S + \frac{1}{Da}\right] = 0 \qquad (2)$$

$$\frac{\partial u}{\partial t} = \vartheta\frac{\partial^2 u}{\partial r^2} + \frac{1}{r}(\vartheta - S)\frac{\partial u}{\partial r} - \frac{u}{r^2}\alpha^2 \qquad (3)$$

Where:

$$\alpha^2 = \vartheta + S + \frac{1}{Da}$$

Subject to the following dimensionless initial and boundary conditions:

$$t \le 0:\ u = 0 \text{ For all } 0 \le r \le \lambda \qquad (4)$$

$$t > 0:\ u = 1 \text{ at } r = 1 \qquad (5)$$

$$t > 0:\ u = \lambda\theta \text{ at } r = \lambda \qquad (6)$$

The solution of Eq. (3) can be obtained using the Laplace transformation (LP) with respect to t define as

$$\bar{u}(r,s) = \int_0^\infty u(r,t)e^{-st}dt,\quad s > 0 \qquad (7)$$

Where s is the Laplace parameter, taking LP of Eq. (3) we have

$$\frac{d^2\bar{u}}{dr^2} + \frac{1}{r}\left(1 - \frac{S}{\vartheta}\right)\frac{d\bar{u}}{dr} - \frac{\bar{u}}{r^2}\frac{\alpha^2}{\vartheta} - \frac{s}{\vartheta}\bar{u} = 0 \qquad (8)$$

With the following boundary condition in the Laplace domain

$$\bar{u} = \frac{1}{s} \text{ at } r = 1 \qquad (9)$$

$$\bar{u} = \frac{\lambda\theta}{s} \text{ at } r = \lambda \qquad (10)$$

Eq. (8) which is linear partial differential equation (LPDE) can be as

$$\bar{u} = \bar{u}_h r^{S/2\vartheta} \qquad (11)$$

to the following homogeneous Bessel equation (HBE)

$$\frac{d^2\bar{u}_h}{dr^2} + \frac{1}{r}\frac{d\bar{u}_h}{dr} - \frac{\bar{v}_h}{r}\left[\frac{S}{\vartheta}r^2 + G\right] = 0 \qquad (12)$$

The solution of Eq. (12) is

$$\bar{u}_h = C_1 I_G(rH) + C_2 K_G(rH) \qquad (13)$$

Where:

I_G Is the G[th] order modified Bessel function of the first kind.

K_G Is the G[th] order modified Bessel function of the second kind.

$$G = \left[\frac{1}{4}\left(\frac{S}{\vartheta}\right)^2 + \frac{\alpha^2}{\vartheta}\right]^{1/2}$$

$$H = \sqrt{\frac{s}{\vartheta}}$$

Substituting Eq. (13) into Eq. (11) we have

$$\bar{u} = \left[C_1 I_G(rH) + C_2 K_G(rH)\right] r^{\frac{S}{2\vartheta}} \quad (14)$$

Using the boundary condition (9) and (10) the constant C_1 and C_2 are obtained as shown below.

$$C_1 = \frac{\left[K_G(\lambda H) - \lambda\theta K_G(H)\lambda^{-S/2\vartheta}\right]}{s\left[I_G(H)K_G(\lambda H) - I_G(\lambda H)K_G(H)\right]},$$

$$C_2 = \frac{\left[I_G(\lambda H) - \lambda\theta I_G(H)\lambda^{-\frac{S}{2\vartheta}}\right]}{s\left[I_G(\lambda H)K_G(H) - I_G(H)K_G(\lambda H)\right]}$$

Eq. (14) is to be inverted to determine the velocity in the time domain. We use the numerical procedure used in (Jha and Apere 2010) which is based on the Riemann-sum approximation. Any function in the Laplace domain *s* can be inverted to the time-dependent domain using the following equation:

$$u(r,t) = \frac{e^{\varepsilon t}}{t}\left[\frac{1}{2}\bar{u}(r,\varepsilon) + \mathrm{Re}\sum_{k=1}^{N}\bar{u}\left(r, \varepsilon + \frac{ik\pi}{t}(-1)^k\right)\right] \quad (15)$$

Where Re is the real part of the imaginary number $i = \sqrt{-1}$, N is the number of terms used in the Riemann-sum approximation, and ε is the real part of the Bromwich contour that is used in inverting Laplace transforms. The accuracy of the Riemann-sum approximation approach depends largely on the value of ε and the truncation error dictated by$N$. For faster convergence, the value of ε must be selected so that the Bromwich contour encloses all the branch points. Hence, for faster convergence, the best value of εt that satisfied the result is 4.7 as in the work of (Tzou. 1997).

2.1 Skin Friction

The skin friction (SF) τ (between fluid layers) defined by $r\frac{\partial}{\partial r}\left(\frac{\bar{u}}{r}\right)$ is obtained by diff Eq.(15) with respect to r

$$\tau_i = r\left(\frac{\partial\bar{u}}{\partial r}\right) = \frac{e^{\varepsilon t}}{t}\left[\frac{1}{2}\bar{u}_1(r,\varepsilon) + \mathrm{Re}\sum_{k=1}^{N}\bar{u}_1\left(r, \varepsilon + \frac{ik\pi}{t}(-1)^k\right)\right] (16)$$

Where:

$$\bar{u}_1 = \left[C_1 I_{G+1}(rH) - C_2 K_{G+1}(rH)\right] H r^{\frac{s}{2\vartheta}} + \frac{s}{2\vartheta} r^{\frac{s}{2\vartheta}-1}\left[C_1 I_G(rH) + C_2 K_G(rH)\right] \quad (17)$$

And

I_{G+1} Is the $(G+1)^{\text{th}}$ order modified Bessel function of the first kind.

K_{G+1} Is the $(G+1)^{\text{th}}$ order modified Bessel function of the second kind.

The SF at the outer surface of the inner cylinder and that at the inner surface of the outer cylinder can then be obtained by substituting $r = 1$ and $r = \lambda$ respectively in Eq. (17) as follows.

$$(\bar{u}_1)_{r=1} = \left[C_1 I_{G+1}(H) - C_2 K_{G+1}(H)\right] H + \frac{s}{2\vartheta}\left[C_1 I_G(H) + C_2 K_G(H)\right] \quad (18)$$

$$(\bar{u}_1)_{r=\lambda} = \left[C_1 I_{G+1}(\lambda H) - C_2 K_{G+1}(\lambda H)\right] H\lambda^{\frac{S}{2\vartheta}} + \frac{s}{2\vartheta}\lambda^{\frac{S}{2\vartheta}-1}\left[C_1 I_G(\lambda H) + C_2 K_G(\lambda H)\right] \quad (19)$$

2.2 Steady State

For the steady-state velocity distribution u_s. The expression is obtained using the following ODE

$$\frac{d^2 u_s}{dr^2} + \frac{1}{r}\left(1 - \frac{S}{\vartheta}\right)\frac{du_s}{dr} - \frac{u_s}{r^2}\frac{\alpha^2}{\vartheta} = 0 \quad (20)$$

Using the following transformation variable:

$$u_s = \bar{u}_s r^{S/2\vartheta} \quad (21)$$

Eq. (20) became HBE as

$$\frac{d^2\bar{u}_s}{dr^2} + \frac{1}{r}\frac{d\bar{u}_s}{dr} - \frac{\bar{u}_s}{r^2}M^2 = 0 \quad (22)$$

Where:

$$M^2 = \frac{S^2}{4\vartheta^2} + \frac{\alpha^2}{\vartheta}$$

Eq. (22) is the standard Euler's equation, and its solution can be written as

$$\bar{u}_s = C_3 r^M + C_4 r^{-M} \tag{23}$$

Substituting Eq. (23) in (21) we have the u_s to be

$$u_s = C_3 r^{S/2\vartheta + M} + C_4 r^{S/2\vartheta - M} \tag{24}$$

Where the constant C_3 and C_4 are obtained using the boundary condition (5) and (6) as shown below

$$C_3 = \frac{\lambda\theta - \lambda^{S/2\vartheta - M}}{\lambda^{S/2\vartheta + M} - \lambda^{S/2\vartheta - M}}$$

$$C_4 = \frac{\lambda^{S/2\vartheta + M} - \lambda\theta}{\lambda^{S/2\vartheta + M} - \lambda^{S/2\vartheta - M}}$$

2.3 Skin Friction for the Steady State Velocity

The dimensionless SF for the steady state velocity u_s which is given as $\tau_s = r\frac{d}{dr}\left(u_s/r\right)$ is obtained as a result of diff Eq. (24) with respect to r.

$$\tau_s = r\frac{d}{dr}\left(\frac{u_s}{r}\right) = C_3\left(\frac{S}{2\vartheta} + A - 1\right)r^{\frac{S}{2\vartheta}+A-1} + C_4\left(\frac{S}{2\vartheta} - A - 1\right)r^{\frac{S}{2\vartheta}-A-1} \tag{25}$$

The steady state SF at the outer surface of the inner cylinder $(r=1)$ and that at the inner surface of the outer cylinder $(r=\lambda)$ can then be obtained from Eq. (25) respectively as follows.

$$\tau_s(r=1) = C_3\left(\frac{S}{2\vartheta} + M - 1\right) + C_4\left(\frac{S}{2\vartheta} - M - 1\right) \tag{26}$$

$$\tau_s(r=\lambda) = C_3\left(\frac{S}{2\vartheta} + M - 1\right)\lambda^{\frac{S}{2\vartheta}+A-1} + C_4\left(\frac{S}{2\vartheta} - M - 1\right)\lambda^{\frac{S}{2\vartheta}-A-1} \tag{27}$$

RESULTS AND DISCUSSION

In order to get a physical insight into the problem, we design a MATLAB program to compute and generate the graphs for the velocity and the SF.

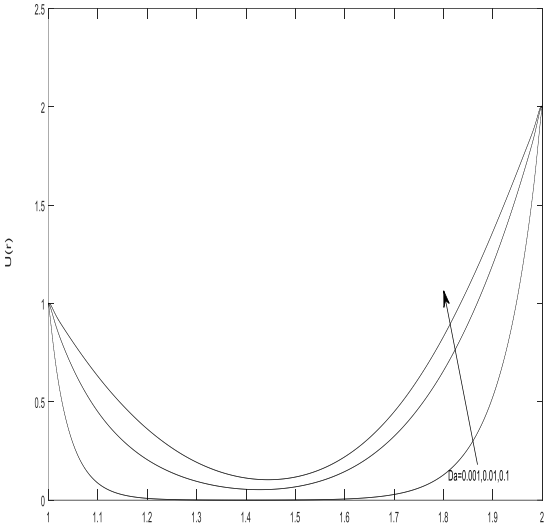

Fig 2: velocity profiles for different values of Da, when $\lambda = 2,\ \theta = 1.0, S = 0.5,\ \vartheta = 1.5, t = 0.02$

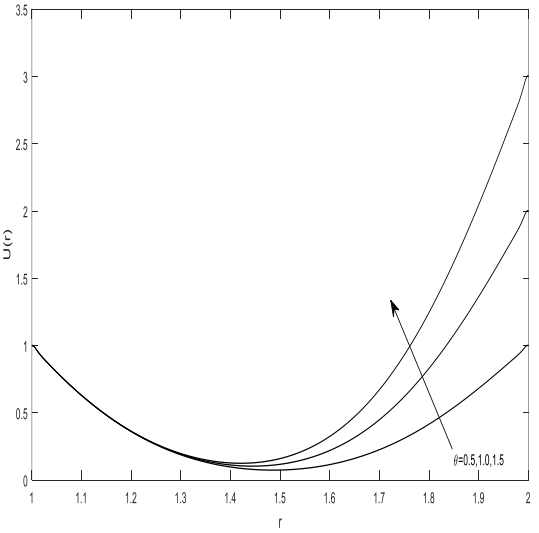

Fig 3: velocity profile for different values of θ when

$\lambda = 2, Da = 0.1, \vartheta = 1.5, t = 0.02, S = 0.5$

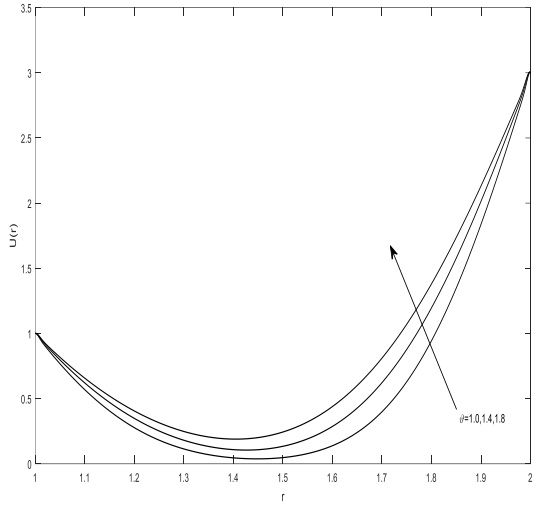

Fig 4: *Velocity profile for different values of* ϑ *, when* $S = 0.5$ *and* $\lambda = 2, \theta = 1.5, t = 0.02, Da = 0.1$

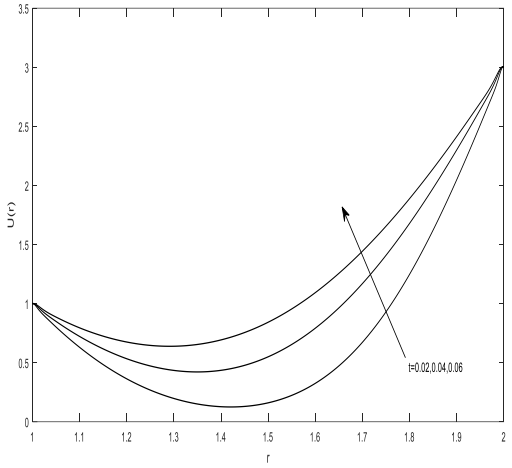

Fig 5: *Velocity profile for different values of time t, for* $S = 0.5$ *and* $Da = 0.1, \vartheta = 1.5, \theta = 1.5$

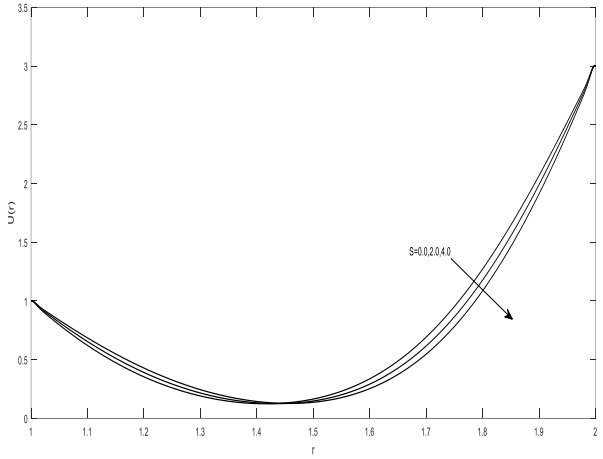

Fig 6: *Velocity profile for different values of* S *,* $t = 0.02$ *and* $Da = 0.1, \vartheta = 1.5, \theta = 1.5$

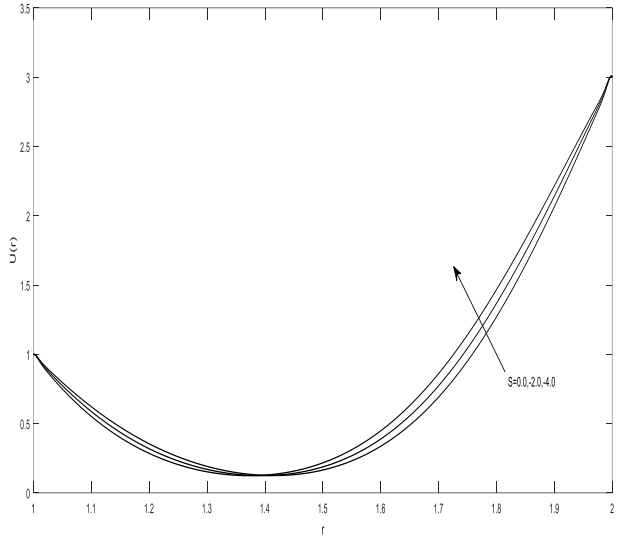

Fig 7: *Velocity profile for different values of* S *,* $t = 0.02$ *and* $Da = 0.1, \vartheta = 1.5, \theta = 1.5$

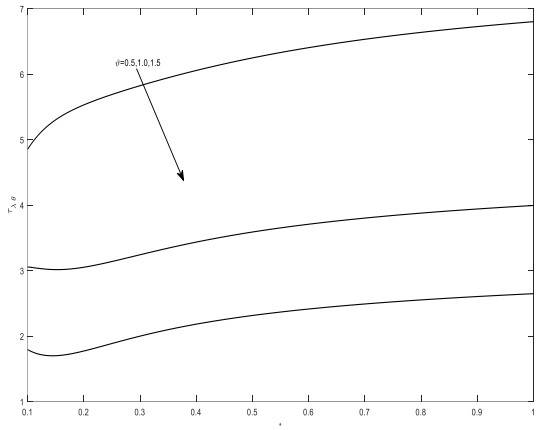

Fig 8: SF on the outer surface of the inner cylinder $r=1$ for different values of ϑ, when $Da=0.1, l=2, \theta=1.5$

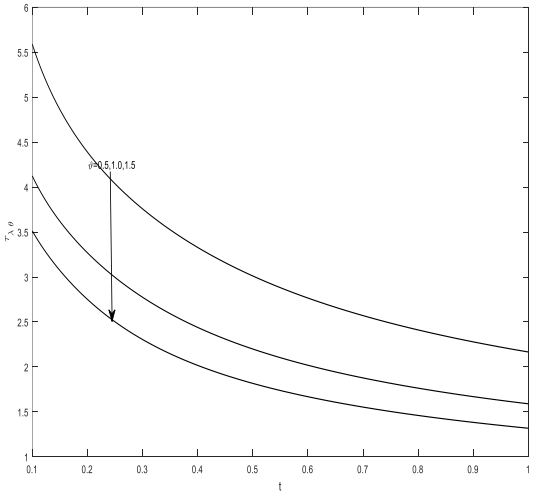

Fig 9: SF on the inner surface of the outer cylinder $r=2$ for different values of ϑ, when $Da=0.1, l=2, \theta=1.5$

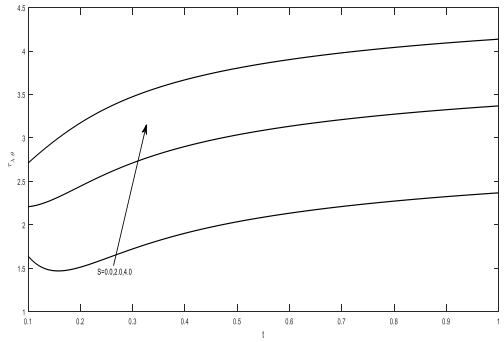

Fig 10: SF on $r=1$ for different values of S, when $Da=0.1, l=2, \theta=1.5$

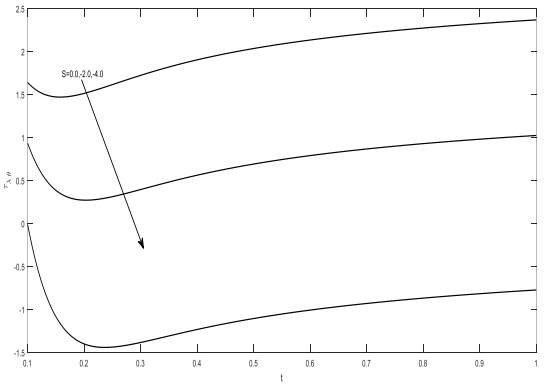

Fig 11: SF on $r=1$ for different values of S, when $Da=0.1, l=2, \theta=1.5$

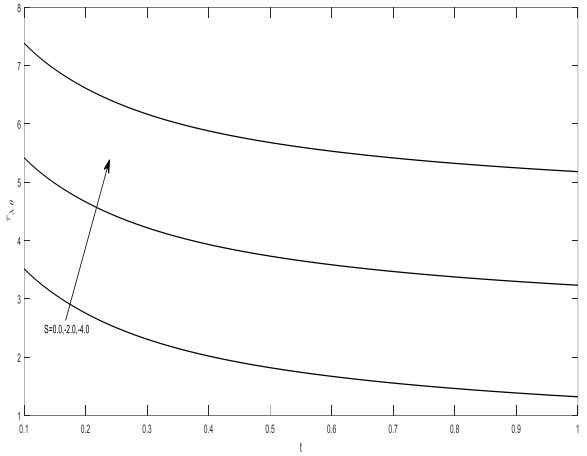

Fig 12: SF on $r=2$ for different values of S, when $Da=0.1, l=2, \theta=1.5$

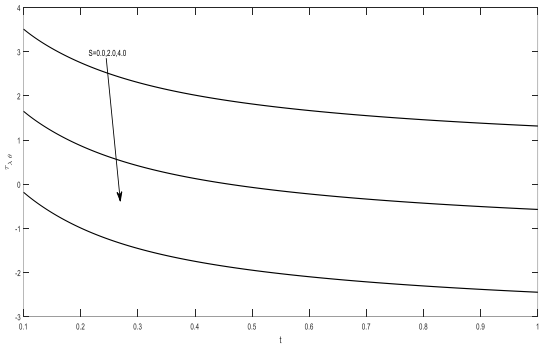

Fig 13: SF on $r=2$ for different values of S, when $Da=0.1, l=2, \theta=1.5$

In Fig.2 velocity profile for different values of Da are shown when $\lambda = 2, \theta = 1.0, t = 0.02,$ and the ratio of viscosity $\vartheta = 1.5$ .Which is a clear case of fluid flow when permeability of medium within the annular region are infinite, the figure reveals that as Da increases, fluid velocity increases because increase in Da means increase in permeability of the medium. A similar behavior is also seen for the velocity in Fig.3 where the effect of θ is been observed on the flow when $\lambda = 2, Da = 0.1, t = 0.02.$ and the ratio of viscosity $\vartheta = 1.5$, the figure shows that as θ increases the velocity also increases as the increase in θ means increase in the temperature. Fig.4 represents a variation of velocity with ratio of viscosity parameter ϑ for fixed values of $\theta = 1.0, Da = 0.1$ and $t = 0.02,$ it has been shown that as ϑ increases then the fluid velocity also increases because increase in ϑ means resistance increase in the flow so it has an increasing effect on the velocity. Similar behavior has been seen in Fig.5 with different values of t and the fixed values of $Da = 0.1, \vartheta = 1.5, \theta = 1.0$ where the velocity increases with increase in time t .

Figs.6 and 7 Shows the profile of the velocity u plotted against r for different values of S , it was discovered from the figures that, an increase in the suction/injection parameters S has a decreasing effect on the velocity whereas the velocity increases as a result of the decrease in the suction/injection parameter $S.$ Figs. 8 and 9 present the variation of the Skin friction at the outer surface of the inner cylinder and that of the inner surface of the outer cylinder respectively, for different values of ϑ and fixed values of $Da = 0.1, l = 2, \theta = 1.$ It is observed that, as the radius of viscosity ϑ increases the SF for both outer surface of the inner cylinder and the inner surface of the outer cylinder decreases and it has a strong effect on the flow. In Figs. 10 and 11 variation of the SF at the inner surface of the outer cylinder is being plotted against time t for fixed values of $Da = 0.1, l = 2, \theta = 1.0$ the effect of the suction/injection parameter S on the Skin friction has been observed, whereas S increase the SF decrease. Figs. 12 and 13 shows the behavior of the SF at the inner surface of the outer cylinder for different values of the suction/injection parameter $S.$ The figure revealed that, as suction/injection parameter S increases the SF decreases, whereas S decreases the SF increases, which is really expected as injection (positive values of S) have a decreasing effect on the flow while suction (Negative values of S) have an increasing effect on the flow.

Table 1
Numerical Values of the velocity obtained using the Riemann sum approximation method and those obtained exactly (for the steady state) at the center of the annulus $(r = 1.5)$.

t	Da	$velocity(u)$ *Riemann Sum*	$Steady\ State(ss)$
0.2	0.001	0.0011	0.0012
	0.01	0.0678	0.2149
	0.1	0.1177	1.0524
0.4	0.001	0.0012	0.0012
	0.01	0.1643	0.2149
	0.1	0.4028	1.0524
2.0	0.001	0.0012	0.0012
	0.01	0.2150	0.2149
	0.1	1.0525	1.0524

The behavior of SF was observed to be similar to that of fluid velocity. To validate the accuracy of the Riemann-sum approximation method, a comparison was made with analytical results for the steady-state case, as presented in Table 1. The results showed excellent agreement between the two methods at large values of time, confirming the accuracy and reliability of the Riemann-sum approximation method employed in this study.

CONCLUSION

The Transient flow formation in concentric porous annuli filled with porous material having variable porosity and formed by two infinitely horizontal concentric cylinders has been investigated. The governing equation has been solved for the velocity and the SF. Riemann sum approximation method has been employed to get the steady state expression for the velocity and the SF. Graphical results for the velocity and the SF showing the effect of various controlling parameters are presented and discussed. It is how ever discovered that the velocity increase with increase in the various controlling parameters at all time. The SF τ is seen to increase with increase in the suction/injection parameter S when $r = 1$ at the outer surface of the inner cylinder. However the SF τ has increases with suction (Negative values of S) and decreases with injection (positive values of S) at the inner surface of the outer cylinder when $r = \lambda$

REFERENCE

Avramenko A.A., Trinov A.I, Shevchuk I.V. (2015). An analytical and numerical study on the start-up flow of slightly rarefied gases in a parallel plate channel and a pipe. J. Porous Media 27,231-246.

Berman A.S. (1958). Laminar flow in an annulus with porous walls. J Appl Phys 29, 71-75.

Deo S. and Srivastava B.G. (2013). Effect of magnetic field on the viscous fluid flow in a channel filled with porous medium of variable permeability. *Journal of Applied Mathematics and Computation.* Vol. 219 pp. 8959-8964

Ebrahim N.H., El-khatib N., and Awang M. (2013). Numerical solution 0f power-law fluid flow through Eccentric annular geometry American journal of Numerical Analysis 1, 1-7.

Jha B.K., Apere C.A. (2013). Time dependent MHD Couette flow in a porous annulus. J Communication in non-linear science and Numerical simulation 188, 1959-1969.

Jha B.K., Apere C.A. (2010). Unsteady MHD Couette flow in an annuli: the Riemann-sum approximation approach. J Phys Soc Jpn 79, 124403/1-3/5

Jha B.K., Apere C.A. (2012). Magnetohydrodynamics transient free-convective flow in a vertical annulus with thermal boundary condition of the second kind J heat transfer 134/042502-1.

Kandasamy A., Nadiminti S.R. (2015). Entrance Region flow in concentric annuli with rotating inner wall for Herschel-Bulkley fluids. Int. J. Appl comput. Math 1, 235-249

Khalil M.F., Kassab S.Z., Adam I.G., Samaha M. (2008). Laminar flow in concentric annulus with a moving core. IWTC 12, 439-452.

Kim, Y.H. (2013). Flow of Newtonian and Non Newtonian fluids in a concentric annulus with a rotating inner cylinder. Korea-Australia Rheolohy, 77-85.

Kuznetsov A.V. (1996). Analytical investigation of the fluid flow in the interface region between a porous medium and a clear fluid in channels partially filled with a porous medium. Appl. Sci. Res. 56, 53-67.

Mishra S.P. and Roy J.S. (1967). Flow of Elasticoviscous Liquid between Rotating cylinders with suction and injection J Phys. Fluids 10, 2300.

Sagir, A.M., M. Abdullahi, and F. Balogun. (2023). An optimal Implicit Block Method for Solutions of the Tumor-Immune Interaction Model of ODEs. Transnational Journal of Mathematical Analysis and Applications. 11(1),45-60. Jyoti Academic Press http://jyotiacademicpress.org

Pantokratoras A., Fang T. (2010). Flow of a weekly conducting fluid in a channel filled with a porous medium. J Transport porous Media. D0I 10.1007/s11242-009-9470-6.

Rothfus R.R., Monrad C.C., Senacal V.E. (1950). Velocity distribution and fluid friction in smooth concentric annuli. J Industrial and Engineering chemistry 4212, 2511-2520.

Srivastava B.G., Deo S. (2013). Effect of magnetic field on the viscous fluid flow in a channel filled with porous medium of variable permeability J Applied Mathematics and Computation 219, 8959-8964.

Tzou D.Y. (1997). Macro to Microscale Heat Transfer: The lagging Behaviors. Washington: Taylor and Francis

Vadasz P. (1993). Fluid flow through heterogeneous porous media in a rotating square channel. J Transport porous media 12, 43-5.

Verma B.K., Datta S. (2012). Flow in an annular channel filled with a porous medium of variable permeability. J Porous Media 15, 891-899.

Verma V.K., Singh S.K. (2014). Flow between coaxial rotating cylinders filled by porous medium of variable permeability. Int J Porous media 54,355-359.

Verma V.K., Singh S.K. (2015). Magnetohydrodynamics flow in a circular channel filled with a porous medium. J Porous Media 189, 923-928.

Yale, I.D., Sa'adu, A., Hamza, M.M. and Bello, Y. (2025). Tranverse Magnetic Field's Impact on Mixed Convection Flow of an Exothermic Fluid over a porous Material – filled Channel. Journal of Basics and Applied Sciences Research, 3(3), 251-260. https://dx.dox.doi.org/10.4314/jobasr.v3i3.27

Appendix A

List of Symbols

R_1 Radius of the inner cylinder

R_2 Radius of the outer cylinder

Da Darcy number

I_m m^{th} order modified Bessel function of the first kind

K_m m^{th} order modified Bessel function of the Second Kind

r' Dimensional radial Coordinate

R Non-dimensional radial coordinate

t Time in non-dimensional form

t' Time in dimensional form

u Fluid velocity in non-dimensional form

u' Fluid velocity in dimensional form

S Suction/Injection Parameter

Appendix B

Greek Symbols

ϑ Ratio of Viscosity

λ Ratio of outer radius and inner radius

ν Kinematic Viscosity of the fluid

θ Dimensionless Temperature

υ_{eff} Effective Kinematic Viscosity of the Porous Medium